


Experimental study on incident wave speed and the mechanisms of deflagration-to-detonation transition in a bent geometry

L. Li¹  · J. Li² · C. J. Teo¹ · P. H. Chang² · B. C. Khoo^{1,2}

Received: 31 May 2016 / Revised: 14 March 2017 / Accepted: 23 March 2017 / Published online: 12 April 2017
© Springer-Verlag Berlin Heidelberg 2017

Abstract The study of deflagration-to-detonation transition (DDT) in bent tubes is important with many potential applications including fuel pipeline and mine tunnel designs for explosion prevention and detonation engines for propulsion. The aim of this study is to exploit low-speed incident shock waves for DDT using an S-shaped geometry and investigate its effectiveness as a DDT enhancement device. Experiments were conducted in a valveless detonation chamber using ethylene–air mixture at room temperature and pressure (303 K, 1 bar). High-speed Schlieren photography was employed to keep track of the wave dynamic evolution. Results showed that waves with velocity as low as 500 m/s can experience a successful DDT process through this S-shaped geometry. To better understand the mechanism, clear images of local explosion processes were captured in either the first curved section or the second curved section depending on the inlet wave velocity, thus proving that this S-shaped tube can act as a two-stage device for DDT. Owing to the curved wall structure, the passing wave was observed to undergo a continuous compression phase which could ignite the local unburnt mixture and finally lead to a local explosion and a detonation transition. Additionally, the phenomenon of shock–vortex interaction near the wave diffraction region

was also found to play an important role in the whole process. It was recorded that this interaction could not only result in local head-on reflection of the reflected wave on the wall that could ignite the local mixture, and it could also contribute to the recoupling of the shock–flame complex when a detonation wave is successfully formed in the first curved section.

Keywords Deflagration-to-detonation transition · S-shaped geometry · Bent tube · Schlieren · Shock–vortex interaction

1 Introduction

The current study addresses the DDT phenomenon in a curved geometry. Curved geometry confinements are commonly used for many industrial applications. In fuel delivery pipelines and mine tunnels, safety issues with respect to strong explosion and detonation are always of major concerns, and thus, the design of such geometries which could suppress these events is of vital importance [1,2]. In addition, curved geometries are also of great interest in the design of engines such as pulse detonation engines (PDE) [3–5] and rotating detonation engines (RDE) [6–9]. For a PDE, to enable a more compact setup, detonation initiation/propagation inside a bent tube has been proposed [10,11]. This approach would not only reduce the PDE overall dimensions, but could also accelerate the detonation initiation process via DDT [12–17]. For an RDE, the detonation waves move tangentially inside an annular combustion chamber, thus eliminating the need for purging, and thus, detonation waves can continuously cycle around the chamber to provide thrust.

Extensive studies have been conducted to investigate the DDT in smooth tubes and obstructed tubes as presented and reviewed in the literature [4,18–21]. The studies of DDT

Communicated by G. Ciccarelli.

This work has been supported by the fund from the National University of Singapore.

✉ L. Li
lilei@u.nus.edu

¹ Department of Mechanical Engineering, National University of Singapore, 5A Engineering Drive 1, 02-02, Singapore, Singapore

² Temasek Laboratories, National University of Singapore, 5A Engineering Drive 1, 09-02 Singapore, Singapore

processes mostly focused on fuel type, mixture composition, geometry confinement, and configuration of obstacles. In summary, the interactions among shock waves, flames, flow turbulence, and boundary layers have been shown to be contributing to flame acceleration and detonation transition. Other factors which include thermal expansion of combustion products, flame–vortex interaction, and instability can play essential roles as well. In addition to the smooth tubes and obstructed tubes, previous literature has also revealed several interesting findings in curved geometries via experiments and numerical simulations. The studies by Frolov et al. [2,22,23] used pressure sensors installed in front of and after two separated U-shaped bent tubes to examine the critical shock wave velocity for a successful shock-to-detonation transition. A shock generator was employed in these studies to form a single shock wave for detonation transition. Through testing in various geometries using stoichiometric propane–air mixture at 1 bar, they found that the minimum speed of the shock wave entering the first bent tube has to be above 850–940 m/s ($0.47V_{CJ} - 0.52V_{CJ}$) in order to attain successful detonation transition through the first bent tube, and 750–850 m/s ($0.42V_{CJ} - 0.47V_{CJ}$) through the second bent tube. It was also reported that the velocity of a shock wave before entering a single bent tube with a larger radius of curvature (50.8 mm) for successful detonation transition increases to 1100 m/s ($0.61V_{CJ}$). From these studies, it is evident that a single U-shaped tube can substantially decrease the minimum shock wave velocity for detonation initiation and transition. Even though the geometry with two U-shaped structures was tested, it was found that the critical velocity required for successful detonation transition was only slightly decreased compared to the case in the single U-shaped geometry. This may be because the two U-shaped tubes are separated by a long distance, and each tube may just interact separately with the incoming wave instead of working in tandem.

Gwak and Yoh [24] examined the effects of bent geometry, obstacles, and initial flame size on DDT via numerical simulation. Different combinations of tube bends with obstacles were tested and the results showed that multiple shock–flame interactions play an important role in assisting DDT. Numerical details further revealed that multiple bends are favorable for detonation transition as compared to a straight and obstructed tube. Gaathaug et al. [25] investigated detonation transition from a single obstacle. It was found that Mach reflection which took place after wave diffraction around the obstacle could lead to a local explosion. The local explosion was observed to originate in a layer between the flame and the wall and then initiate the DDT process at a location far behind the leading edge of the flame.

The objective of this study is to further explore the lower velocity limit of incident waves for a successful DDT process using bent geometries. To achieve this, an S-shaped geome-

try is thus proposed in this study to investigate whether the critical shock wave velocity for a successful DDT process can further be decreased if there are more than one bent tube connected closely to each other (so as to achieve an S-shaped geometry). In the experiment, a shock wave followed by a flame zone is initiated using a spark plug, which is different from that applied for the shock-to-detonation transition study in [2,22,23]. Specifically, this initiation approach is similar to those employed in the real engine applications. So this investigation could also shed light on the dynamics regarding the initiation of detonation in PDEs and RDEs. In addition, the optical measurement techniques that are employed in this study to visualize the mechanism(s) that could trigger the onset of detonation have seen only limited application in the literature for such curved geometries.

2 Experimental setup

A valveless detonation driver section was used to carry out the experiments. The driver section was outlined in detail in a previous paper [15]. A round cross-sectional S-shaped tube is added to the outlet of the existing straight detonation driver section as the new test chamber of interest. For the S-shaped geometry, the inner radius is 25.4 mm and the outer radius is 76.2 mm. Mixtures of ethylene and air were continuously supplied from the manifold upstream. Fifteen round orifice obstacles with a blockage ratio of 43% were installed in the straight tube to accelerate the flame speed to a certain degree before advancing into the S-shaped tube. Owing to the flame acceleration process, a leading shock wave can be formed in the front and it can then interact with the geometry separately before the following flame catches up. Based on our experiments, the number of obstacles employed in the present study is not sufficient to accelerate a flame to a detonation wave. As shown in Fig. 1, three different ignition locations were used. Due to the stochastic nature of flame acceleration, leading shock waves can thus be obtained within a wide speed range below CJ velocity. Six pressure sensors (PCB113B24) were installed before and after the S-shaped tube to monitor the incident and transmitted wave velocities, respectively.

The experiments were conducted in a single-shot firing mode at room temperature and pressure (303 K, 1 bar). Air was continuously supplied upstream, and ethylene was injected by two fuel injectors (Alternative Fuel System Inc.) to the manifold 400 mm upstream of the ignition spark for ethylene–air premixing. The injection period of ethylene was set to 0.3 s. With the means to control the air venting velocity inside the geometry, it is arranged to be sufficiently long for the mixture to completely fill the whole tube. The air flow rate was controlled by a choked nozzle which has an uncertainty of 0.89%. The fuel injection rate was monitored by a fuel flow rate meter (Alicat Scientific) which has an uncertainty

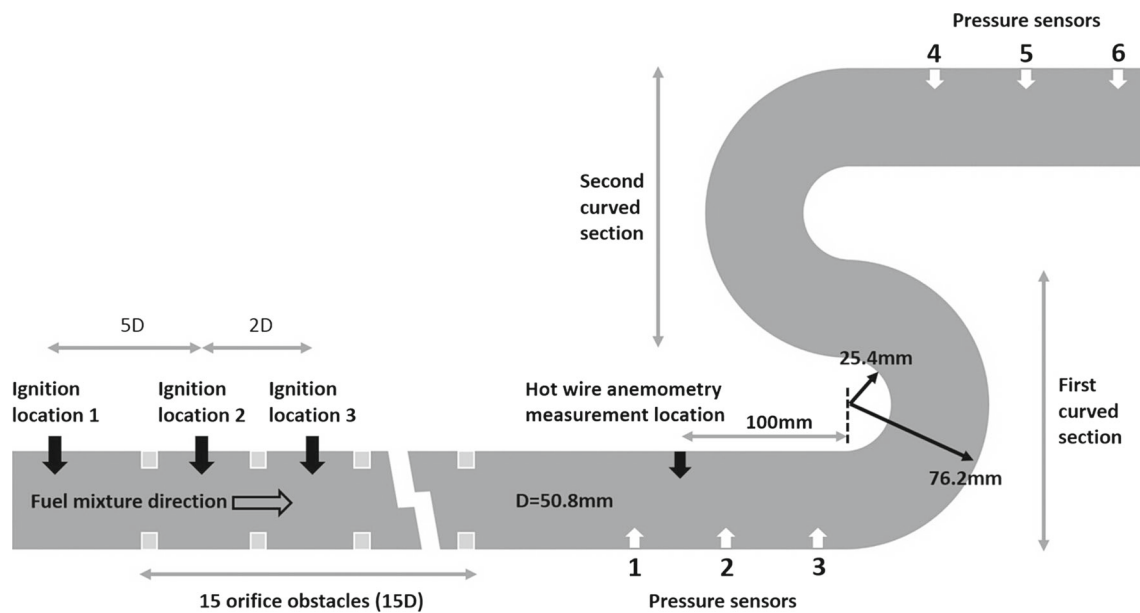


Fig. 1 Schematic of the S-shaped detonation tube

of 0.8%. So this single-shot testing mode has an overall equivalence ratio uncertainty of approximately 1.2%. The ignition spark was fired immediately after the injection period. In order to make sure that the flow mixture inside the tube has attained a statistically homogeneous turbulent condition after 0.3 s of the fuel injection period, hot wire anemometry has been employed at 100 mm upstream of the S-shaped tube inlet (Fig. 1) to measure the initial flow and quantify the turbulence intensity before and after the fuel injection. By analyzing the velocity change before ignition, it was found that the mean mixture flow velocity inside the tube can become statistically homogeneous in 0.1 s after injection. The turbulence intensities before fuel injection and during the period between 0.1 and 0.3 s after fuel injection were calculated to be 7.1 and 7.2%, respectively, thereby indicating that the flow is fully developed for ensuing experiments. After ignition, the burnt gas left behind would be purged away by the continuous air flow, and then, the system is ready for the subsequent firing.

3 Optical diagnostics

In order to visualize and ascertain how DDT can be achieved at such a low inlet wave speed, an optically accessible channel with an identical geometry from plan view direction, as shown in Fig. 2, was designed and installed to replace the previous S-shaped tube. A Z-type Schlieren system was set up for wave observation. The size of each concave mirror is 0.15 m, and the focal length of each concave mirror is 1.2 m. The concave mirror is approximately 0.9 m away from the optical accessible window section. To keep track of the

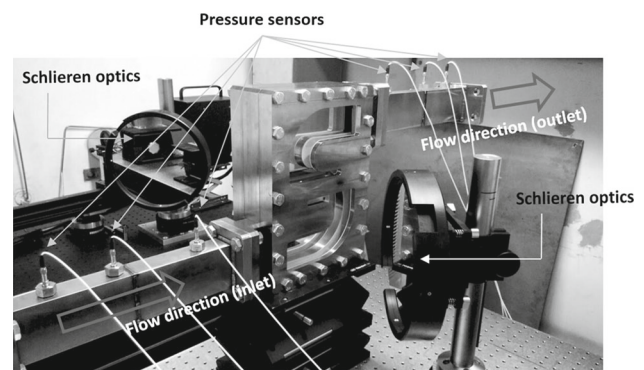


Fig. 2 Optically accessible detonation channel

dynamic changes of the waves, a high-speed camera (Photron SA-Z) was used together with a Nikon 70–300 mm lens. A high camera framing rate at 210,000 Hz with a reduced resolution of 384 pixels \times 160 pixels and a low camera framing rate at 80,000 Hz with a relatively better resolution of 640 pixels \times 360 pixels were both applied during the recording. The exposure time was set to 250 ns for each frame captured. Similarly, pressure sensors were installed ahead of and behind the S-shaped channel to monitor the wave velocity. Alternatively, the velocity can be determined by measuring the difference in wave locations between two consecutive imaging frames. The channel cross section is 20 mm (width) \times 50.8 mm (height). To synchronize the high-speed imaging system with the incoming shock wave, a digital delay (Stanford Research Systems DG645) was used to send a trigger signal to the camera once a voltage rising signal was received from the first pressure sensor upstream.

For the imaging of photographs, a horizontal knife edge placed in the middle of a circular hollow adaptor was utilized. This permitted visualization of the vertical density gradient and also differentiation of large density variations in all directions by the circular edge on the adaptor. Consequently, the strong shock wave moving in all directions in this curved geometry can be imaged as a clear dark line all along the wave front. A flame front moving in the vertical direction with a relatively small density gradient can be imaged as a bright line due to the pressure drop after the flame. As for the decoupled distributed flame regions behind the leading shock, since their density gradients are generally small

and non-uniform, they can be visualized as distributed dark regions with several bright spots within.

4 Minimum shock wave velocity for successful DDT

Experimental results based on pressure sensor signals are shown in Fig. 3. From the results, we can see that, except for the misfire shots (activation of the spark plug that does not lead to ignition or ignition failure before the pressure sensor location) and other shots with detonation as inlet waves, DDT can be observed for 90% of cases. When the results are sorted according to the inlet shock wave speed as shown in Fig. 4, it was found that the minimum propagating speed of the incident shock wave that was capable of successfully initiating detonation through this S-shaped tube was approximately 500 m/s compared to 850–1100 m/s observed in the U-shaped tube [23]. Note that this velocity is substantially lower than that needed for detonation initiation in straight tubes, and it is relatively easy to obtain within a short tube length. Successful cases with even lower inlet velocities have also been achieved, as can be observed from the sparsely distributed points at the bottom of Fig. 4. Note that each velocity shown in Fig. 4 is the average velocity between the two adjacent pressure sensors (sensor 2 and sensor 3), and the point mid-way between the two sensors is 50 mm upstream of the S-shaped tube inlet. A typical pressure data plot for successful DDT is shown in Fig. 5. In this example, the inlet shock wave speed is approximately 600 m/s and the sharp pressure peak together with the transmitted wave velocities downstream of the S-shaped tube indicate clear detonation features.

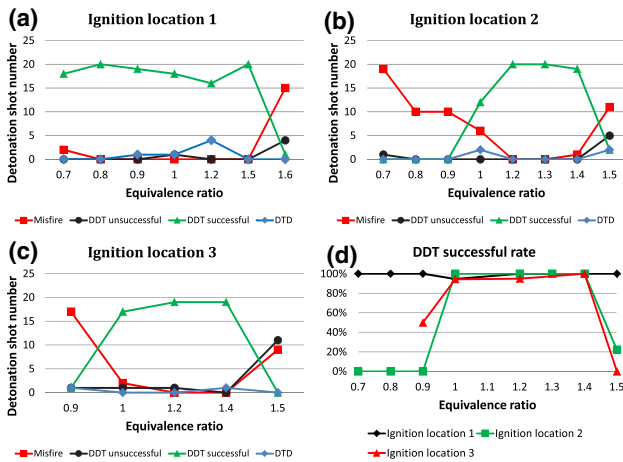
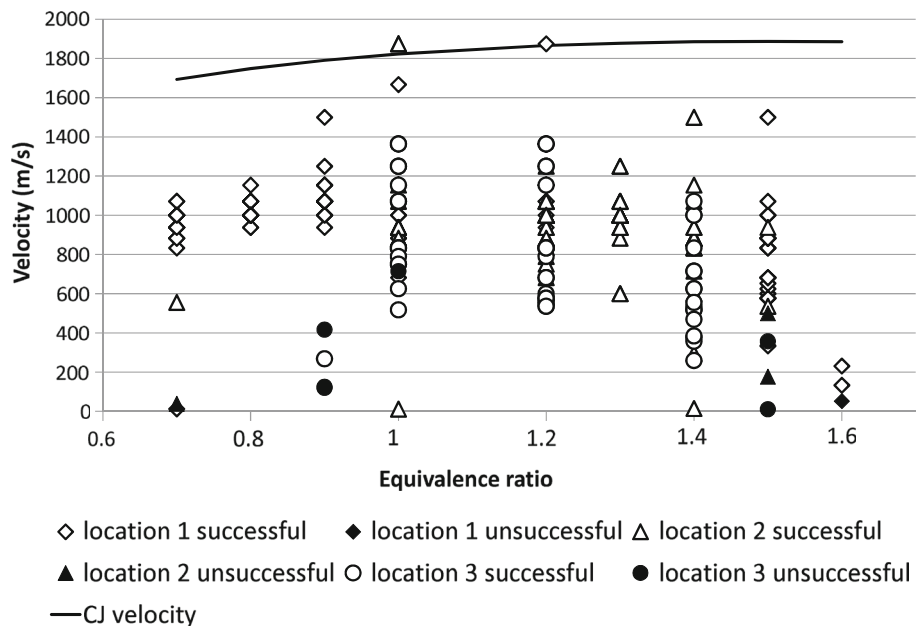


Fig. 3 a–c Experimental results at ignition locations from 1 to 3. d DDT success rate = (DDT successful)/(DDT successful + DDT unsuccessful). DTD means inlet wave is detonation and outlet wave is also detonation

Fig. 4 Inlet shock wave velocity for successful and unsuccessful DDT



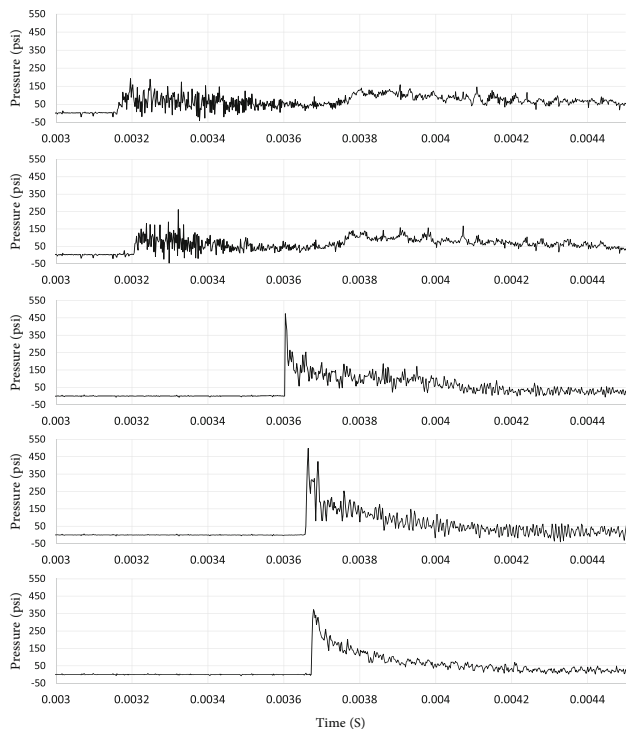


Fig. 5 Pressure sensor records of one DDT example (two sensors No. 2, 3 upstream and three downstream No. 4, 5, 6). $V_{45} = 2631$ m/s and $V_{56} = 2142$ m/s

5 Mechanisms of DDT in the S-shaped tube

To study the dynamics leading to DDT at such low wave velocities, high-speed Schlieren photography was focused on both the first and the second curved section. In order to better relate the optical measurement results with the testing conditions in Sect. 4, an overview is summarized in Table 1. As shown in Fig. 6, two distinct patterns of shock reflection phenomenon can be identified in both the first curved section (cases 1 and 2) and the second curved section (cases 3 and 4). The inlet velocities shown in Fig. 6 (1, 2) were calculated

based on the location differences of the leading shock waves in two consecutive image frames. The inlet velocities in the other two images were calculated based on the inlet pressure sensors. From the two patterns identified in the first curved section, case 1 shows a Mach reflection configuration comprising a Mach stem, an incident wave, a reflected wave, and a shear layer near the wall. The Mach stem was observed to be small during its propagation. This is because of the continuous change of the wall angle along the first U-shaped path so that the contact angle between the wall and the incident wave can be kept relatively small. As a result, the transition from regular reflection to Mach reflection is delayed, and the generated Mach stem cannot grow rapidly at such a small contact angle. Behind the incident shock wave, a train of weak compression waves can be found. For a faster and stronger incident shock wave as shown in case 2, a localized explosion which is responsible for the onset of detonation was observed. From the two wave patterns identified in the second curved section, case 3 shows successful detonation transition with a local explosion occurring in the second curved section. The inlet wave velocity, in this case, is close to the minimum velocity summarized in Sect. 4. As for the case when a local explosion has occurred in the first curved section, the wave that went into the second curved section would experience a decoupling process due to the geometry diffraction, and a subsequent recoupling process as shown in case 4, which will be further discussed below.

5.1 Local explosion at the first curved section

To examine the detailed process of the local explosion, Fig. 7 shows typical high-speed Schlieren imaging of the local explosion in the first curved section. An explosion core was first observed near the small Mach stem due to the continuous compression phase. It was found that the explosion onset location always coincided with one strong compression wave behind the leading shock. It is thus possible that this strong compression wave provides further compression to the highly

Table 1 An overview table of selected typical detonation shots with successful detonation transitions

Shot number	Inlet velocity (m/s)	Equivalence ratio	Observed initiation location
651	1276	1.0	First curved section
721	1200	1.5	First curved section
731	869	1.5	Downstream of the second curved section
761	857	1.5	Second curved section
764	869	1.5	N/A
770	765	1.5	N/A
799	1032	1.3	First curved section
800	1310	1.5	First curved section
844	582	0.9	Second curved section

Here, N/A refers to the cases in which the camera was not taking pictures at the location where DDT took place

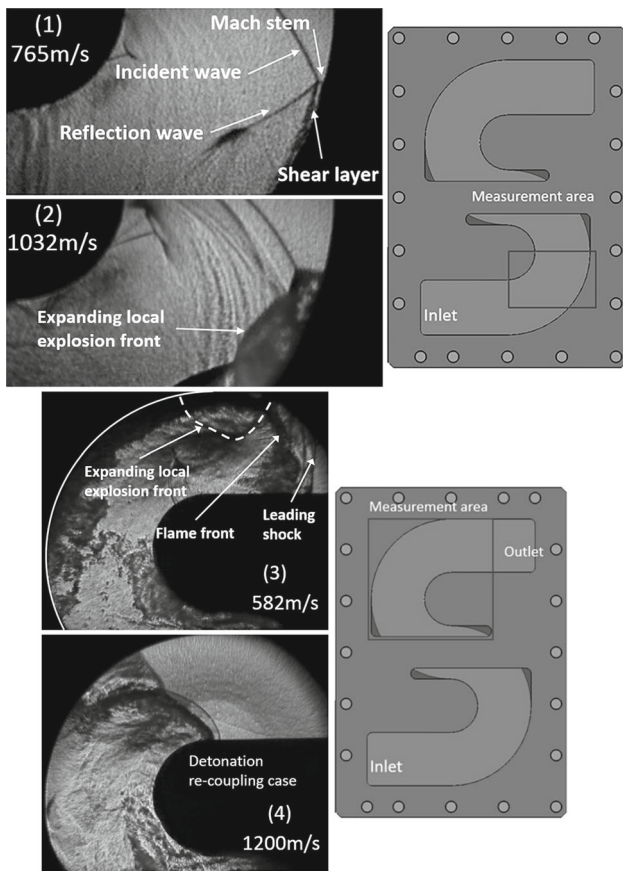


Fig. 6 Different shock and detonation reflection patterns inside the S-shaped channel of several typical successful DDT cases. The image shot numbers for case 1 to case 4 are listed as shot number 770, 799, 844, and 721. See Table 1. Number in each image indicates the inlet velocity

reactive gas near the wall and acts as a trigger for the onset of the local explosion. After the onset of explosion, the small core instantaneously expanded outwards and caught up with the leading Mach stem. The subsequent images for the same experimental firing, which are not presented here, indicate that this local explosion which was induced by the Mach stem constituted the sole cause for the successful detonation transition, while the original flame front rapidly died out due to the lack of unburnt mixture which had been completely consumed by this explosion before the flame arrived.

As this local explosion was found responsible for DDT in the first curved section, we also investigated the critical conditions for such a local explosion to occur. The graph of shock wave and flame front locations at different imaging frames of Fig. 7 are plotted in Fig. 8. Here, and elsewhere, T_0 refers to the reference time of the first image frame in a series as the phenomenon evolved with time. Figure 9 shows a sample image to demonstrate the method for locating shock/flame fronts inside the channel. Each image frame was overlaid onto the three-dimensional file of the S-shaped tube using

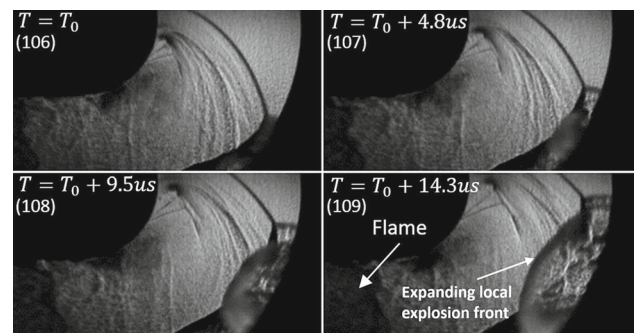


Fig. 7 High-speed imaging of the local explosion at the first curved section (210,000 frames/s). Number in parenthesis shows the frame number (shot number 800 as referenced in Table 1)

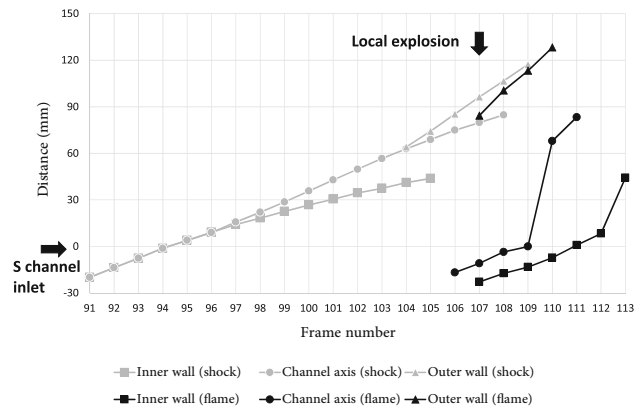


Fig. 8 Graph of location versus frame number for local explosion in the first curved section. Local explosion at frame 107 according to Fig. 7 (shot number 800 as referenced in Table 1)

modeling software to fit the channel geometry so that the size of each pixel could be calibrated. Then, after identifying the locations of the wave fronts, the distances can be calculated based on the angles and distances measured directly from the software, thus to minimize any possible error. The fronts of shock and flame at the inner wall, channel axis, and outer wall were all identified to calculate their running distances from the inlet.

According to Fig. 8 (shot number 800) before the S-shaped tube inlet, the shock wave was moving at a speed of 1310 m/s along both the inner wall and the channel axis. Owing to the continuous compression at the outer wall and the shock diffraction at the inner wall, it is clearly observed that the shock wave velocity along both the channel axis and the outer wall gradually became faster than that along the inner wall. It was calculated that the shock wave was moving at a much faster average speed of 2451 m/s at the outer wall than that of 837 m/s at the inner wall before the local explosion. With the shock wave being accelerated to such a high speed, a local explosion was then triggered at frame 107 near the outer wall. Immediately after the local explosion, the speed of the detonation wave further increased to approximately

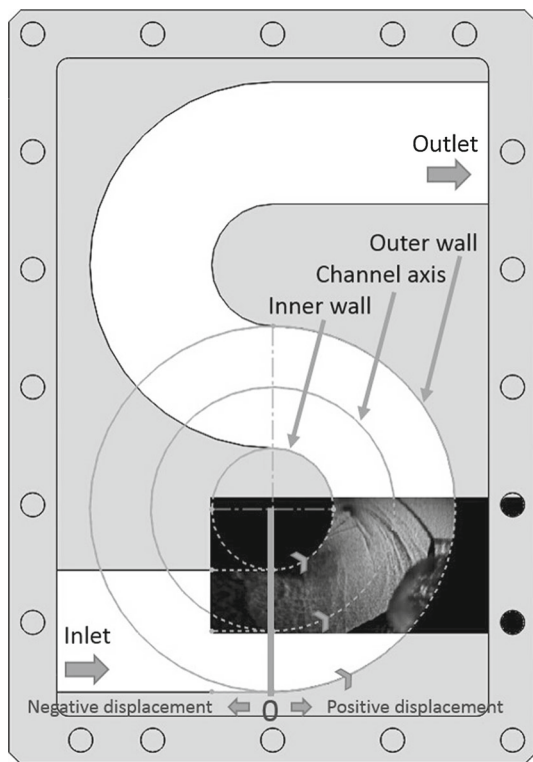


Fig. 9 Schematic of the images post-processing method

Table 2 The detonation shots with local explosion found at the first curved section

Shot number	Inlet velocity (m/s)	Shock wave velocity at outer wall before local explosion (m/s)	Equivalence ratio
725	1143	2311	1.5
726	1213	2553	1.5
763	1037	2212	1.5
783	1185	2438	1.4
784	1201	2227	1.4
793	1241	2449	1.3
794	1126	2265	1.3
799	1032	2244	1.3

3070 m/s. Then, the explosion front was observed to expand radially inwards and subsequently hit the channel axis and the inner wall at frames 109 and 112, respectively, with both the velocities attained at higher than 2500 m/s temporarily.

To summarize the critical conditions for local explosion in the first curved section from several other similar cases (see Table 2), it was discovered that the local explosion only took place when the shock wave velocity was larger than approximately 1000 m/s before going into the curved channel, or 2200 m/s after being accelerated at the channel outer wall. It was also found that the critical velocity has a general increasing trend with increasing equivalence ratio. To compare with

the previous studies, it was found that this critical velocity of 1000 m/s is comparable with the range of 850–1000 m/s that was summarized in Frolov et al. [23].

It should be noted that all cases in Fig. 6 experienced successful DDT according to the pressure sensor signals further downstream. The local explosion which was originated from the continuous compression of shock waves on the outer wall was found to be responsible for the detonation transition at higher than 1000 m/s. However, the underlying mechanisms for DDT below 1000 m/s, as shown in case 1, are still unclear. Next, we shall focus on the second curved section for further investigation.

5.2 Local explosion at the second curved section

Figure 10 shows a typical DDT process which has a similar inlet wave condition with that in case 1 in Fig. 6 as they both have inlet velocity below 1000 m/s. The inlet wave velocity was measured to be 857 m/s which was not strong enough to initiate a local explosion in the first curved section. After propagating through the whole S-shaped channel, the leading shock wave and the corresponding transverse wave were sweeping between the channel walls. In frames 80 and 82 of Fig. 10, the trailing distributed flame region as originally shown in frames 76 and 78 transformed into a flame front with a clear preceding shock wave. This transformation was due to the acceleration of the flame region after temperature increase from multiple reflections of the leading shock and the compression waves along the path. In frame 84, a small explosion core can be clearly identified at the channel exit. It rapidly transformed into an intensive local explosion and expanded rapidly outwards which resembles the process in Fig. 7. To look for the origin of this local explosion, when the flame accelerated toward the vertical direction as depicted from frame 78 to 80, it was confined by the outer boundary wall which formed a decreasing contact angle between the outer wall and the flame front. A link between the experimental findings and the gradient mechanism [26] may exist which can then provide an explanation for the origin of the local explosion. During the subsequent compression phase of the flame front on the outer wall, the small amount of unburnt mixture which is confined by the wall and the flame front could form a gradient in temperature and induction time. An explosion core was subsequently formed at $75 \mu\text{s}$ (frame 82) near the intersection location between the flame and the boundary wall, where it may have minimum induction time due to the prolonged compression along the wall. As the explosion core expanded toward the unburnt mixture which was confined by the wall and the flame front, it subsequently was able to couple with the multiple pressure wave fronts generated from reactions in the induction time gradient to result in a strong expanding explosion wave. As a consequence, the explosion wave caught up with the leading shock and suc-

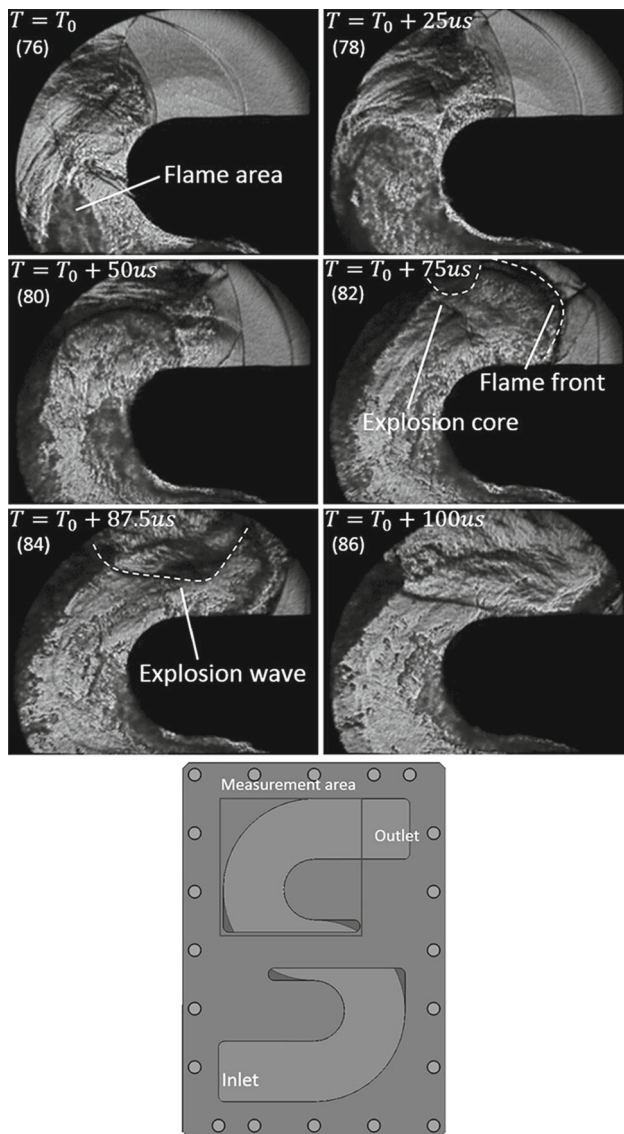


Fig. 10 High-speed imaging of the localized explosion at the second curved section (80,000 frames/s) (shot number 761 as referenced in Table 1)

cessfully formed a self-sustaining detonation wave according to the velocity calculated from the downstream pressure sensors. Note that even though the local explosions were also observed here, they were directly initiated from the accelerating flame front instead of the leading shock wave, as shown in the first curved section in Fig. 7. This is because the leading shock wave before propagating into the second curved section was the diffracted shock wave in the first curved section. As the shock strength in the first curve was not strong enough to initiate detonation, the diffracted shock going into the second curved section would be even more attenuated in strength to achieve transition.

According to the figures and descriptions, this second curved section is thus acting as a second stage for flame

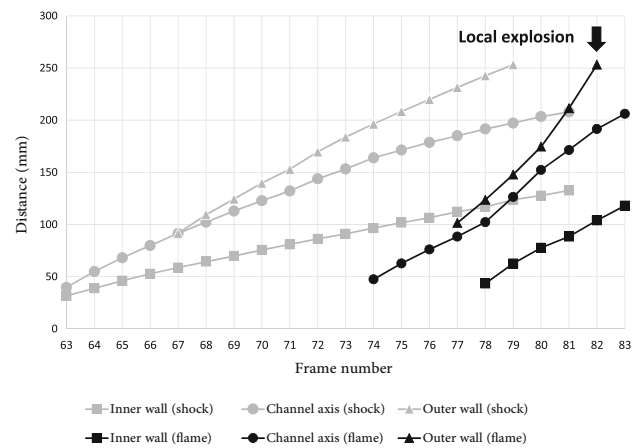


Fig. 11 Graph of location versus frame number for local explosion in the second curved section. Local explosion at frame 82 according to Fig. 10 (shot number 761 as referenced in Table 1)

acceleration which could then enable an even lower critical velocity for DDT. More evidence of how local explosion was initiated are exemplified in Fig. 11. Near the second curved section inlet (frame 67), the outer wall shock wave was moving at approximately 1438 m/s and the inner wall shock wave was moving at approximately 457 m/s. After the flame front has shown up in the camera field of view, the flame at the outer wall was accelerated all the way up from 1775 to 3348 m/s before a local explosion was triggered. As limited by the camera field of view, the time of the flame catching up with the leading shock wave was not recorded. But it can be estimated from the frame number of the intersection point after extending the respective lines in this figure.

5.3 Shock–vortex interaction

Even though detonation transition through localized explosion appears to be a universal phenomenon in many different geometry confinements, the preparation stage for detonation onset sometimes could vary significantly. A few mechanisms which include the interactions among flames, shock waves, flow turbulence, and boundary layers have been identified to be responsible for flame acceleration and wave amplification from previous literature. Apart from these, another one which involves the interaction between the vortex near the diffraction shear layer and the reflected wave has been observed to play a significant role in assisting detonation transition in the present geometry.

5.3.1 Local head-on reflection of the reflected wave

Figure 12 shows a case with inlet shock wave velocity of 832 m/s which was not sufficiently strong to initiate a local explosion in the first curved section. At T_0 , a regular reflec-

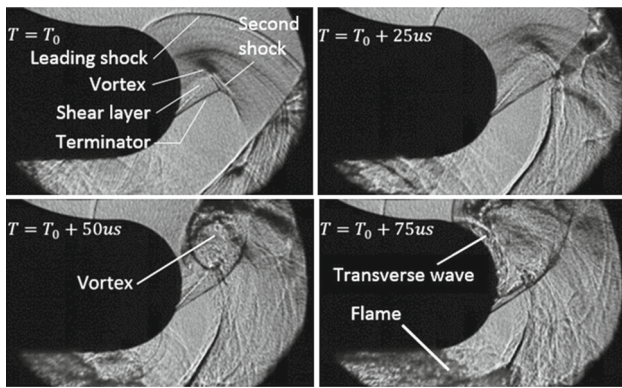


Fig. 12 Interaction of vortex and reflected wave in the first curved section (80,000 frames/s) (shot number 764 as referenced in Table 1)

tion configuration can be observed near the outer wall of the channel. At the location near the inner wall, a shear layer, the terminator of the Prandtl–Meyer expansion fan, and a second shock wave can be clearly identified [27]. At $25 \mu\text{s}$, the reflected wave was approaching the vortex near the shear layer. Owing to the differences in the flow direction, velocity, and pressure between the vortex and the approaching reflected wave, the reflected wave was wrinkled to develop a convex structure toward the vortex. In the next frame of $50 \mu\text{s}$, the wrinkled reflected wave has completely passed through the vortex and split into two parts. The wave near the bottom moved back into the horizontal channel. The wave on the top has evolved into a curve which reflects the shape of the vortex near the shear layer. This process can help induce flow turbulence at the reflected wave front and mix the highly reactive mixture with the less reactive mixture. It can also roll up the wave toward the inner wall to have a head-on reflection at a relatively high velocity. Note that the transverse wave after reflection is shown as a bright line at $75 \mu\text{s}$. Taking the Schlieren knife edge direction into consideration, it represents a negative density gradient from top to bottom which is analyzed to be a possible flame front separating unburnt mixture on the top from the combustion products on the bottom [28]. It is thus suggested that the head-on reflection, which is induced by the shock–vortex interaction can assist DDT by increasing the flow turbulence, mixing the reactive mixture, and igniting the vicinity of the transverse wave before the following decoupled flame catches up and runs by.

The same shock–vortex interaction can also be found in the second curved section, as shown in Fig. 13. To better illustrate the interaction, a graphical representation of the evolution of such shock–vortex interactions in Figs. 12 and 13 is depicted in Fig. 14. It should be pointed out that in some Schlieren images, it is not straightforward to differentiate the flame from the unreacted flow turbulence region as both of them are captured by the digital camera and interpreted as distributed regions with large and continuous density varia-

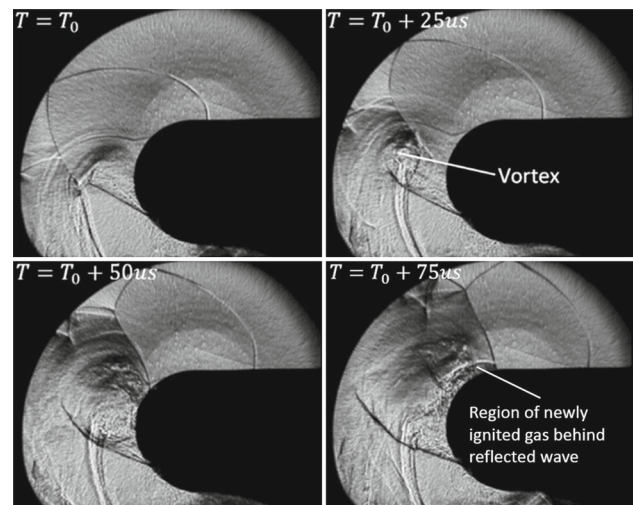


Fig. 13 Interaction of vortex and reflected wave in the second curved section (80,000 frames/s) (shot number 731 as referenced in Table 1)

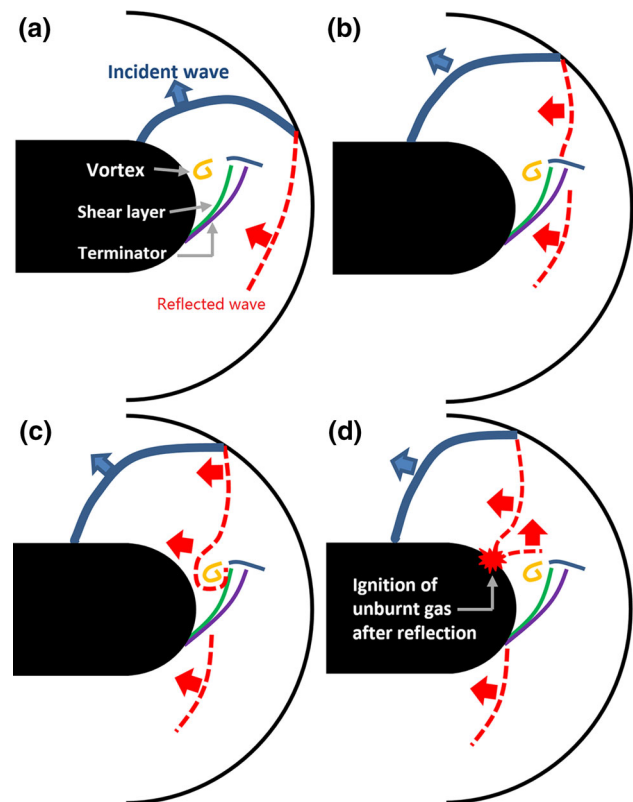


Fig. 14 Schematic of the shock–vortex interaction

tions. Examples include the regular reflection region near the outer wall in Fig. 12 and the Mach stem in Fig. 7. In order to clarify this issue, planar laser-induced fluorescence (PLIF) will be employed in the next phase of our planned research to further address this problem and verify our hypotheses [29].

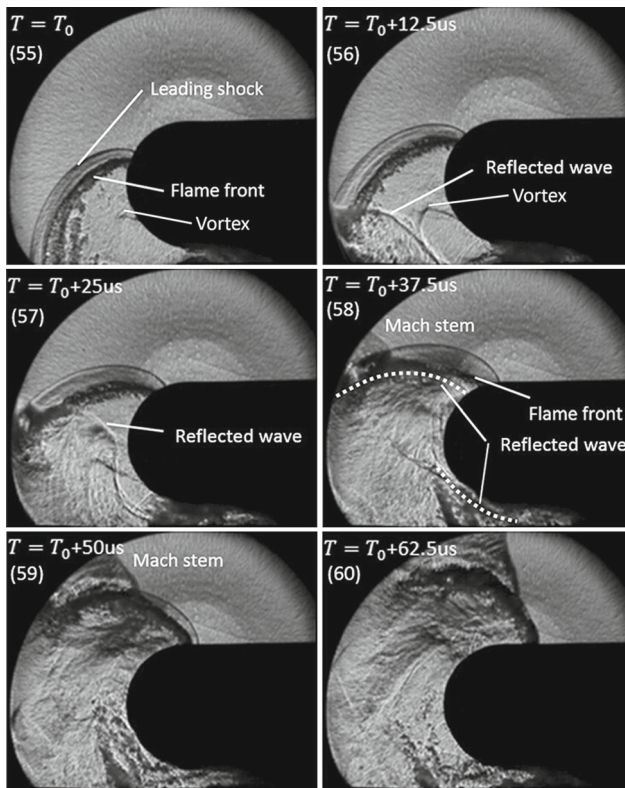


Fig. 15 Shock and flame recoupling caused by the shock–vortex interaction (80,000 frames/s) (shot number 721 as referenced in Table 1)

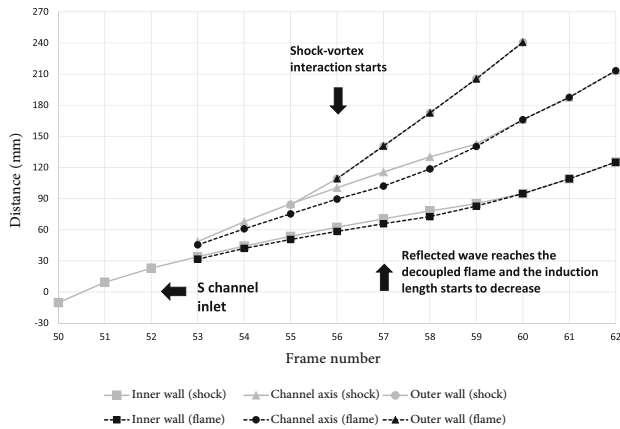


Fig. 16 Graph of location versus frame number for shock and flame recoupling (shot number 721 as referenced in Table 1)

5.3.2 Shock and flame recoupling process

Except for the flow turbulence generation, flame acceleration, and mixture ignition, the interaction between shock and vortex was observed to be crucial for the shock–flame recoupling during detonation reinitiation in the second curved section. An example is shown from Figs. 15, 16, and 17 both qualitatively and quantitatively. When the inlet wave velocity at the S-shaped channel inlet is larger than 1000 m/s, an over-

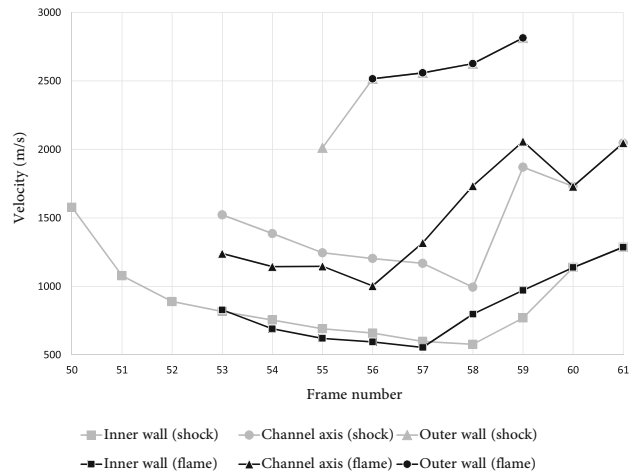


Fig. 17 Graph of velocity versus frame number for shock and flame recoupling (shot number 721 as referenced in Table 1)

driven detonation wave can be observed in Fig. 15 at the inlet of the second curved section due to the occurrence of a local explosion in the first curved section. Figure 17 indicates that the velocity of the inner shock wave was 1577 m/s before moving into the curved section. It immediately decreased to 577 m/s at frame 58 after experiencing a sudden diffraction in the second curved section. Because of this diffraction, a clear induction zone between the flame and shock wave can be observed at frame 55. As the diffraction continues, the distance becomes more obvious from frame 55 to 57, suggesting that the incoming detonation wave was subjected to temporary attenuation. At the same time, a reflected wave initiated from the outer wall started to bend toward the direction of the shear-layer-induced vortex near the inner wall. The bent wave was then approaching the decoupled flame at frame 57 and finally coincided completely with the flame at frame 58. The flame was subsequently found to accelerate and catch up with the decoupled shock wave from frame 57. This is due to the forced coupling between the flame and the reflected shock wave which enhanced the chemical reaction rate at the flame front. The distance between the leading shock wave and the decoupled flame thus started to decrease until they finally coupled with each other at frame 60. The effect from the shock–vortex interaction is shown more evidently in Fig. 17 as the velocity of the flame front at the inner wall was recorded with an increase from 555 to 798 m/s, even though it was still under diffraction. The pressure sensors at further downstream revealed that a self-sustaining detonation wave was reinitiated successfully after the recoupling process. It is important to note that when the decoupled flame catches up near the inner wall, the main triple point and the transversely propagating detonation have yet to reach that location. Therefore, it suggests that the shock–vortex interaction made the sole contribution to the recoupling of the

decoupled shock and flame even though the velocities of both dropped to less than 600 m/s during diffraction, thus ensuring a self-sustaining detonation wave at the outlet of the S-shaped channel.

There is another possible mechanism to assist detonation transition which should be mentioned here, even though it has not been addressed in the present research. According to Frolov et al. [23], the DDT process could only be successful if the marginal detonation near the outer wall at the outlet can expand to homogenize the entire wave front. By conducting experiments in such an S-shaped geometry, the weak and diffracted part of the wave front at the outlet of the first curved section could in turn be compressed and strengthened at the second. As a result, what it can achieve could be a wave with a relatively uniform strength which is then favorable for detonation transition. But a longer propagation channel which should also be optically accessible is needed at the outlet of this S-shaped geometry if such a phenomenon is to be observed and the role of wave homogeneity is to be assessed. Another point to notice is the narrow rectangular channel geometry used for optical diagnostics, which is different from the circular tube geometry in Sect. 4. So differences in cell width would be anticipated between them [30]. However, since the channel width is comparable with the cell width in the present test condition (20 mm), which would not be taken as too narrow for the detonation wave tested, the differences of test results and the mechanisms summarized for channels could still be applied in tube geometries in Sect. 4.

From these results, we see that by adding an extra curved section to form an S-shaped geometry, it can act as a two-stage DDT device which can further decrease the critical shock wave velocity for a successful detonation transition. So installation of such a device could be beneficial to the applications such as PDE and RDE, such that detonation can be easily achieved in an even more compact setup. To analyze the influence from the shape of the geometry, according to Lee [14], the multiple reflections of small transverse waves on the wall are reported to be essential for detonation onset as transverse waves can be progressively amplified through multiple bounces back and forth between the walls. It is also revealed by Polley et al. [31] that the multiple reflections of the incident wave on the geometry confinement can play a vital role for detonation transition. It could thus be inferred that geometries which ensure multiple reflections between waves and wall can increase their effectiveness as a detonation onset and transition device. However, in the present study, due to the continuous change of deviation angle in the S-shaped geometry and relatively late transition from regular reflection to Mach reflection as indicated in Fig. 6, the triple points could not reflect between the confinement walls but are always restrained near the outer wall of the S-shaped chamber. Even though DDT is still shown to be able to occur at a relatively early stage in the present study, it is in fact

due to the prolonged continuous compression phase which can directly increase the strength of the Mach stem and local perturbations in the absence of multiple reflections, such that a local hot spot could initiate from the outer wall and act as the trigger for detonation transition through local explosion.

6 Conclusions

In this study, the minimum velocity for successful DDT process inside an S-shaped geometry has been examined, and the detailed mechanisms have been investigated. The experiments used spark plug ignition, which could generate a leading incident shock and a trailing flame front to address DDT phenomenon in engine applications. It was observed that a shock wave with velocity as low as 500 m/s can transit to detonation in this particular S-shaped tube. This velocity is a substantial decrease from the critical velocity reported in the existing literature using a single U-shaped tube. High-speed Schlieren photography was employed to reveal the mechanisms for such a low inlet velocity. Velocity information was also extracted to summarize the critical conditions. It was found that due to the continuous compression phase near the geometry outer wall, local explosions, which are responsible for detonation transition, can be initiated. The approximate critical velocities for the incident shock wave and the shock wave at the outer wall are 1000 and 2200 m/s, respectively. It is found that if a leading shock can move faster than 1000 m/s, or if the shock wave at the outer wall can move faster than 2200 m/s, the local explosion can originate from the leading shock wave in the first curved section. If the velocities were below the critical values, then the local explosion would be triggered from the accelerating flame in the second curved section or even further downstream. In addition, the interaction between the vortex near the shear layer and the reflected wave from the outer curve was found to play an important role in detonation transition and reinitiation. This interaction is capable of inducing a head-on reflection of the wrinkled reflected wave on the wall to ignite the local mixture during flame acceleration. It is also responsible for the recoupling of the shock wave and the flame when a detonation wave formed in the first curved section has partially decayed during diffraction in the second curved section.

Generally, the S-shaped geometry confinement was found to be a very effective enhancement device for DDT. Since this study only focused on the detonation transition mechanisms in two curved sections, influences arising from the geometry dimensions, such as the curvature radius and the cross-sectional area, have not been addressed. Next, more efforts will be devoted to different geometry dimensions to investigate how DDT could be affected. Additionally, PLIF will be employed in the next stages to differentiate between combustion and non-combustion regions in Schlieren results [29].

References

1. Frolov, S.M., Aksenov, V.S., Basevich, V.Ya.: Initiation of detonation in sprays of liquid fuel. *Adv. Chem. Phys.* **24**(7), 71–79 (2005)
2. Frolov, S.M., Aksenov, V.S., Shamshin, I.O.: Shock wave and detonation propagation through U-bend tubes. *Proc. Combust. Inst.* **31**(2), 2421–2428 (2007)
3. Kailasanath, K.: Review of propulsion applications of detonation waves. *AIAA. J.* **39**(9), 1698–1708 (2000)
4. Oran, E.S., Gamezo, V.N.: Origins of the deflagration-to-detonation transition in gas-phase combustion. *Combust. Flame* **148**(1–2), 4–47 (2007)
5. Roy, G.D., Frolov, S.M., Borisov, A.A., Netzer, D.W.: Pulse detonation propulsion: challenges, current status, and future perspective. *Prog. Energy Combust. Sci.* **30**(6), 545–672 (2004)
6. Bykovskii, F.A., Zhdan, S.A., Vedernikov, E.F.: Continuous spin detonation in annular combustors. *Combust. Explos. Shock Waves*. **41**(4), 449–459 (2005)
7. Bykovskii, F.A., Zhdan, S.A., Vedernikov, E.F.: Continuous spin detonations. *J. Propul. Power* **22**(6), 1204–1216 (2006)
8. Bykovskii, F.A., Zhdan, S.A.: Current status of research of continuous detonation in fuel-air mixtures. *Combust. Explos. Shock Waves*. **51**(1), 21–35 (2015)
9. Kindracki, J., Wolanski, P., Gut, Z.: Experimental research on the rotating detonation in gaseous fuels-oxygen mixtures. *Shock Waves* **21**(2), 75–84 (2011)
10. Kudo, Y., Nagura, Y., Kasahara, J., Sasamoto, Y., Matsuo, A.: Oblique detonation waves stabilized in rectangular-cross-section bent tubes. *Proc. Combust. Inst.* **33**(2), 2319–2326 (2011)
11. Nakayama, H., Moriya, T., Kasahara, J., Matsuo, A., Sasamoto, Y., Funaki, I.: Stable detonation wave propagation in rectangular-cross-section curved channels. *Combust. Flame* **159**(2), 859–869 (2012)
12. Ciccarelli, G., de Witt, B.: Detonation initiation by shock reflection from an orifice plate. *Shock Waves* **15**(3–4), 259–265 (2006)
13. Frolov, S.M.: Detonation initiation and DDT: experiments and numerical simulations. In: *Proceedings of the 5th International Seminar on Fire and Explosion Hazards, Edinburgh* (2007)
14. Lee, J.H.S.: *The Detonation Phenomenon*. Cambridge University Press, Cambridge (2008)
15. Li, J., Teo, C.J., Lim, K.S., Wen, C., Khoo, B.C.: Deflagration to detonation transition by hybrid obstacles in pulse detonation engines. In: *49th AIAA/ASME/SAE/ASEE Joint Propulsion Conference*. San Jose, AIAA Paper 2013–3657 (2013)
16. Lu, F.K., Meyers, J.M., Wilson, D.R.: Experimental study of a pulse detonation rocket with Shchelkin spiral. In: *Proceedings of the 24th International Symposium on Shock Waves, Beijing* (2005)
17. Shchelkin, K.I., Troshin, Y.K.: *Gasdynamics of Combustion*. Akad. Nauk SSSR, Moscow (1963)
18. Ciccarelli, G., Dorofeev, S.: Flame acceleration and transition to detonation in ducts. *Prog. Energy Combust. Sci.* **34**(4), 499–550 (2008)
19. Gamezo, V.N., Ogawa, T., Oran, E.S.: Numerical simulations of flame propagation and DDT in obstructed channels filled with hydrogen-air mixture. *Proc. Combust. Inst.* **31**(2), 2463–2471 (2007)
20. Lee, J.H.S.: Initiation of gaseous detonation. *Ann. Rev. Phys. Chem.* **28**, 75–104 (1977)
21. Silvestrini, M., Genova, B., Parisi, G., Leon Trujillo, F.J.: Flame acceleration and DDT run-up distance for smooth and obstacles filled tubes. *J. Loss Prev. Process Ind.* **21**(5), 555–562 (2008)
22. Frolov, S.M., Aksenov, V.S., Shamshin, I.O.: Reactive shock and detonation propagation in U-bend tubes. *J. Loss Prev. Process Ind.* **20**(4–6), 501–508 (2007)
23. Frolov, S.M., Aksenov, V.S., Shamshin, I.O.: Propagation of shock and detonation waves in channels with U-shaped bends of limiting curvature. *Russ. J. Phys. Chem. B* **2**(5), 759–774 (2008)
24. Gwak, M., Yoh, J.J.: Effect of multi-bend geometry on deflagration to detonation transition of a hydrocarbon-air mixture in tubes. *Int. J. Hydrogen Energy* **38**(26), 11446–11457 (2013)
25. Gaathaug, A.V., Vaagsaether, K., Bjerketvedt, D.: Experimental and numerical investigation of DDT in hydrogen-air behind a single obstacle. *Int. J. Hydrogen Energy* **37**(22), 17606–17615 (2012)
26. Zel'dovich, Y.B., Librovich, V.B., Makhviladze, G.M., Sivashinsky, G.I.: On the development of detonation in a nonuniformly pre-heated gas. *Astronaut. Acta* **15**, 313–321 (1970)
27. Skews, B.W.: Shock diffraction on rounded corners. In: *Proceedings of the Third Australasian Conference on Hydraulics and Fluid Mechanics, Sydney* (1968)
28. Bhattacharjee, R.R.: *Experimental Investigation of Detonation Re-initiation Mechanisms Following a Mach Reflection of a Quenched Detonation*. Masters Thesis, University of Ottawa, Ottawa (2013)
29. Boeck, L.R., Kellenberger, M., Rainsford, G., Ciccarelli, G.: Simultaneous OH-PLIF and schlieren imaging of flame acceleration in an obstacle-laden channel. *Proc. Combust. Inst.* **36**(2), 2807–2814 (2017)
30. Ishii, K., Monwar, M.: Detonation propagation with velocity deficits in narrow channels. *Proc. Combust. Inst.* **33**(2), 2359–2366 (2011)
31. Polley, N.L., Egbert, M.Q., Petersen, E.L.: Methods of re-initiation and critical conditions for a planar detonation transforming to a cylindrical detonation within a confined volume. *Combust. Flame* **160**(1), 212–221 (2013)